2021 43rd Annual International Conference of the
IEEE Engineering in Medicine & Biology Society (EMBC)
Oct 31 - Nov 4, 2021. Virtual Conference

Prediction Deviants with Varying Degrees Induce Separable Error-related EEG Features *

Jiayuan Meng[#], Jiao Liu[#], Hao Wang, Minpeng Xu*, *Senior Member, IEEE,* Dong Ming, *Senior Member, IEEE*

***Abstract*—Error-related potential (ErrP) usually emerges in the brain when human perceives errors and is believed to be a promising signal for optimizing brain-computer interface (BCI) system. However, most of the ErrP studies only focus on how to distinguish the correct and wrong conditions, which is not enough for the BCI application in real scenarios. Therefore, it is necessary to study the ErrPs induced by the prediction deviants with varying degrees, concurrently test the separability of such EEG features. To this end, electroencephalogram (EEG) data of twelve healthy subjects were recorded when they participated in a direction prediction experiment. There are three prediction -deviant conditions in it, i.e., correct prediction, 90°deviant, 180° deviant. Event-related potential and inter-trial coherence were analyzed. Consequently, the error-related negativity (ERN) and N450 component in FCZ were significantly modulated by the degrees of prediction deviants, especially in the low-frequency band (<13Hz). Moreover, single-trial classification was adopted to test the separability of these features; the averaged accuracies between any two conditions were 87.75%, 85.25%, 64.79%. This study demonstrates the prediction deviants with varying degrees can induce separable ErrP features, which provide a deeper understanding of the ErrP signatures for developing BCIs.**

Keywords—Error-related Potential (ErrP); Brain-computer interface(BCI); Varying Degrees; Discriminative Canonical Pattern Matching (DCPM); Prediction Deviants.

I. INTRODUCTION

Brain-computer interface (BCI) is a rising technology, which can detect and translate the activities of the central nervous system into computer instructions [1, 2]. Currently, P300 [3], steady-state visual evoked potential (SSVEP) [4, 5], event-related desynchronization (ERD) [6] are the most used electroencephalogram (EEG) signals for BCIs. However, these signals are far from enough for naturally expressing the brain's intentions. More EEG signals, especially those triggered by top-down cognitive processes, remain investigated for developing and optimizing BCIs.

Error-related potential (ErrP) is an endogenous EEG signal emerging when the brain perceives errors [7, 8]. It is made up of error-related negativity (ERN) [9], error positivity (Pe) [10], and some other subcomponents, such as N200, N450, etc. [7]. ErrP can be theoretically explained by the predictive coding, which proposes the brain is essentially a prediction machine, and human perceptions are shaped by learning from the deviants between predictions and sensory inputs [11, 12]. Other than the signals evoked solely by external stimuli, ErrP is triggered by prediction deviants, reflecting the voluntary mental activity of the brain[8]. Thus, ErrP is a promising EEG signal for developing BCIs. It is necessary to have a deeper understanding of ErrP to make better use of it.

Up to now, a typical ErrP application in the BCI system is to work as an automatic error correction signal, improving both the reliability and speed of P300/SSVEP-based BCI spellers [13, 14]. Recent studies further highlight the crucial role of ErrP in developing neuroadaptive technology, i.e., training the computer to learn from errors, enabling it to adapt to an estimate of its operator's mindset automatically [9, 15]. The neuroadaptive technology places greater demands on the understandings of ErrP; thus, more detailed ErrP studies are conducted, such as categorizing different kinds of errors [16], combining ErrPs with asynchronous BCIs [17], etc. However, most of the studies only distinguish the ErrPs in entirely correct and wrong conditions. It remains unknown what signatures would be when the prediction deviants induce ErrPs with varying degrees; it also remains unknown whether these EEG features are separable or not.

This study intends to investigate ErrP signatures induced by prediction deviants with varying degrees and probe into the separability of these EEG features. For this, a direction prediction experiment was conducted, which contained three prediction-deviant conditions, i.e., correct, 90° deviant, 180° deviant. Consequently, ERN and N450 in FCZ were significantly modulated by the deviant degrees, especially in the low-frequency band (<13Hz). The discriminative canonical pattern matching algorithm was adopted for classification; the average accuracies between any two conditions were 87.75%, 85.25%, 64.79%, respectively. The results illustrate the prediction deviants with varying degrees can induce separable ErrP features for BCI use.

II. MATERIALS AND METHODS

A. Participants

Twelve healthy subjects(5 males; 20.8±0.69 years old), who were without psychological or neurological diseases and had normal or corrected to normal vision, participated in this study. The Institutional Review Board at Tianjin University approved experimental procedures involving human subjects. The written informed consent was obtained from all the subjects.

This work is supported by the National Natural Science Foundation of China (No. 81601565， 81630051). Young Elite Scientist Sponsorship Program by CAST (2018QNRC001) and Tianjin Key Technology R&D Program (No. 17ZXRGGX00020).

Jiayuan Meng, Jiao Liu, Hao Wang, Minpeng Xu, Dong Ming are with the college of Precision Instruments & Optoelectronics Engineering, Tianjin University, Tianjin, 300072 China; Minpeng Xu, Dong Ming are in the Academy of Medical Engineering and Translational Medicine, Tianjin University, Tianjin, China. ([#]These authors contributed equally to this work; *the corresponding author to provide phone: 022-27408718; e-mail: minpeng.xu@tju.edu.cn).

B. Experiments

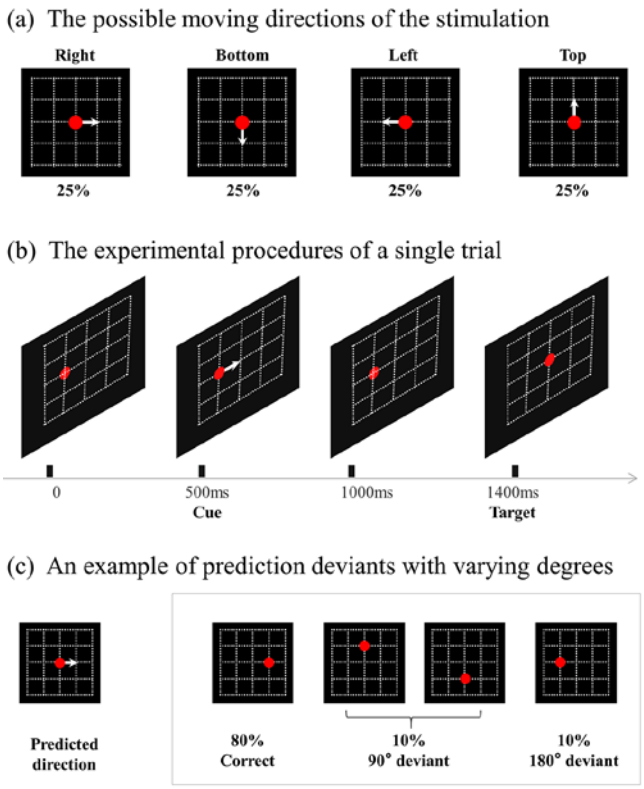

Figure 1. Illustration of experimental design. (a) possible moving directions of the stimulation, which emerged with equal possibility. (b) experimental procedures of a single trail. (c) an example of prediction deviants with varying degrees.

In the direction prediction experiment, the red dot had four possible directions. As figure 1(a) showed, the moving direction with the highest possibility was illustrated by an arrow. The procedures of a single trial were shown in figure 1(b). Specifically, the trial started with a 16×16 grid, a red dot located at a random grid point; 500ms later, a white arrow appeared, indicating the most likely moving direction; after the arrow disappeared, the dot moved to the next grid point, which could lead to three prediction-deviant conditions, i.e., correct prediction, 90° deviant, 180° deviant. A single trial sustained about 1400ms, there were 140 trials in a block. The whole experiment contained 4 blocks. Subjects could rest as long as they want between blocks.

Figure 1(c) is an example showing how to form prediction deviants with varying degrees. To be specific, the predicted direction is formed according to the arrow's indication. Such prediction was reinforced by the large proportion (80%) of correctness, in which the dot did move in the direction the arrow indicated. However, in 14 trials (10%) of each block, the dot moved to deviate 90° (clockwise or counterclockwise) away from the predicted direction, i.e., 90° deviant condition. In another 14 trials (10%) of each block, the dot moved in a completely opposite direction comparing to the predicted one, i.e., 180° deviant condition. In this way, three prediction -deviant conditions were built up. There were totally 56 trials with 90° deviant, 56 trials with 180° deviant, and 448 trials with correct prediction. This study randomly selected 56 trials for the 448 correct trials for further data analysis.

C. Data Recording and pre-processing

The SynAmps2 and Quik-Cap with a 1000Hz sampling rate recorded the EEG signals, hardware-filtered in range of 0~200Hz, and a 50Hz trap filter was applied to the raw data, aiming to remove the power line interference. 64 electrodes were placed on the scalp following the international 10-20 system. The prefrontal lobe and the central electrode were selected as the ground and reference, respectively. Eye-blinks were monitored by signals recorded at FP1 and FP2.

Further, EEG analyzes data were conducted by MATLAB R2017b (MathWorks, MA, USA) with toolbox EEGLAB, and statistical analyzes were carried out on IBM SPSS Statistics 24 (IBM Company, NY, USA). The acquired data were filtered in a range of 0.1~45Hz and resampled to 200Hz. As to data extraction, in each trial, the data in the period of -500ms to 1400ms relative to the target onset was extracted for subsequent analyzes. Moreover, the baseline was corrected using the averaged value calculated from the data 200ms before the target moment.

D. Data Processing and Analysis

The event-related potential (ERP) in FCZ and PZ electrodes were first analyzed to have a general observation of the ErrP signatures. According to the waveform, three typical components, i.e., ERN, Pe, and N450, were selected, and the corresponding temporal windows were showed in table1. The amplitudes of each component were calculated as the mean within the specified time window.

Table 1. Selection of time windows and amplitudes of components

Component	Time window(ms)
ERN	180~230
Pe	270~320
N450	380~430

Then, we analyzed the time-frequency distribution of inter-trial coherence (ITC). The short- time Fourier transform (STFT) should be first calculated as equation (1), in which h(t) is the window function.

$$S(\omega,t)=\frac{1}{2\pi}\int_{-\infty}^{+\infty}e^{-j\omega t}s(\tau)h(\tau-t)d\tau \quad (1)$$

Inter-trial coherence (ITC), which measures phase coherence among trials, was calculated as equation (2). Its value is between 0 and 1; a higher value indicates stronger coherence of the phase in each trial.

$$\mathrm{ITC}(\omega,t)=\frac{1}{N}\left|\sum_{i=1}^{k}\frac{S_i(\omega,t)}{|S_i(\omega,t)|}\right| \quad (2)$$

As to classification, the discriminative canonical pattern matching (DCPM) algorithm [18] was used. It contains three major parts: construction of discriminative spatial patterns, construction of CCA patterns, and pattern matching. EEG data of 24 electrodes (FC3, FC1, FCZ, FC2, FC4, C3, C1, CZ, C2, C4, CP5, CP3, CP1, CPZ, CP2, CP4, CP6, P5, P3, P1, PZ, P2, P4, P6) between 160~630ms of every single trial were selected for classification. For each subject, 44 trials and 10 trials were randomly selected as the training set and testing set under three events, respectively. All the classification accuracies were computed with a 10-fold cross-validation procedure.

III. RESULTS

A. Event-related potential (ERP) analyzes

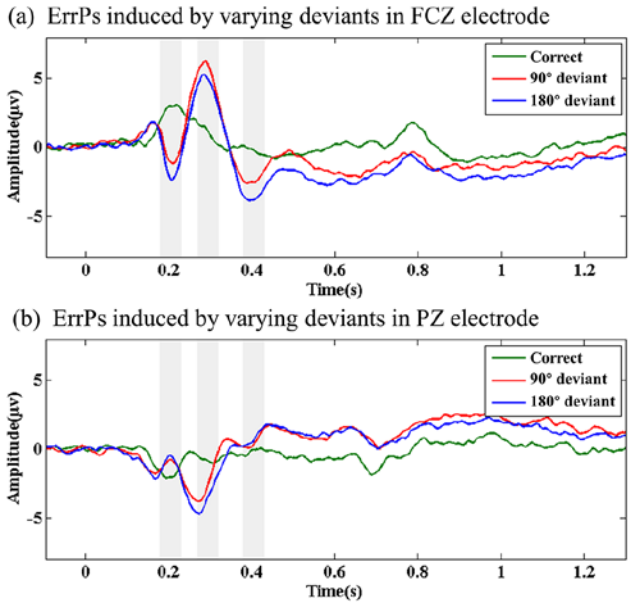

Figure 2. The ErrPs induced by prediction deviants with varying degrees in (a) FCZ, and (b) PZ electrodes.

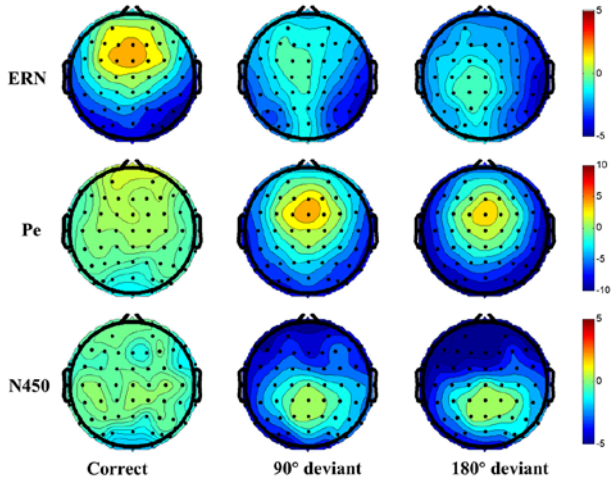

Figure 3. Topographical distribution of the ERN, Pe, and N450 components in correct, 90° deviant，180° deviant conditions.

As figure 2 showed, the ErrPs induced by this direction prediction experiment contained three typical subcomponents, i.e., ERN, Pe and N450. Comparing to the waveforms in PZ, these components are more evident in the FZ electrode. These observations were consistent with previous studies, which reported that ERN is a negative deflection peaking frontal-centrally about 100ms after an error occurs [9]; Pe is a positive wave following ERN and often peaks in central -parietal areas [10]; while other error-related subcomponents, such as N450 often located in the parietal-occipital area [7]. The topographical distributions of the three components were shown in figure 3. These observations not only confirmed the reliability of this study, but also highlighted the typical subcomponents of ErrP, which could be further analyzed.

Based on the above analyzes, one-way repeated analysis of variance (ANOVA) of ERN, Pe, and N450 amplitude were calculated, and Bonferroni correction was applied when necessary. As shown in figure3(a), in FCZ electrode, ERN ($F(2,22)=9.378$, $P= 0.005$), Pe ($F(2,22)=7.431$, $P=0.011$) and N450 ($F(2,22) = 10.000$, $P<0.001$) all revealed significant differences among conditions. In particular, there were statistical significances between 90° and 180° deviant conditions in ERN ($P=0.05$) and N450 ($P=0.001$) amplitude, and the larger the prediction deviant was, the more negative the waveform was.

As to the amplitude of three components in PZ electrode, no statistical significance was found in ERN($F(2,22)=0.251$, $P= 0.780$), Pe ($F(2,22)=2.143$, $P= 0.141$) or N450 ($F(2,22)= 0.882$, $P= 0.428$).

The ERP analyzes demonstrated that the varying degrees of prediction deviants (90° vs. 180°) can modulate the signatures of ErrP, especially the ERN and N450 subcomponents. This result provides new neural evidence supporting a neuronal model of predictive coding accounting for the mismatch negativity, assuming a close association between the degree of prediction deviant and ErrP amplitude [19].

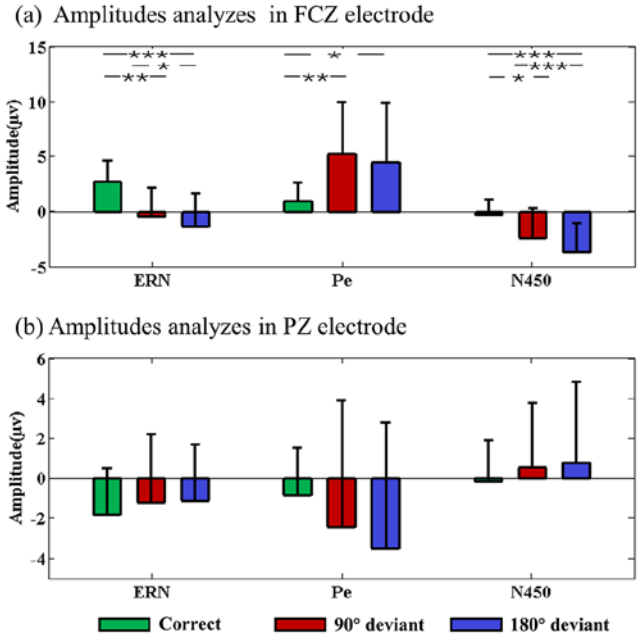

Figure 4. (a) amplitudes analyze in FCZ electrode. (b) amplitudes analyze in PZ electrode. Statistical significance: *0.01<p<0.05, **0.001<p<0.01, ***: p<0.001.

B. Inter-trial coherence (ITC) analyzes

To further probe into the ErrP signatures. This study further analyzed the time-frequency distribution of the ITC. Figure 5(a) showed the time-frequency areas, where there was statistical significance among the three prediction deviant conditions (red areas represent $P<0.005$, while the P-value in white areas was larger than 0.05). Combining such P-value distribution with the ERP analyzes, we calculated the ITC value in the time window of ERN, Pe, and N450. Specifically, in delta beta, the ITCs with deviant were much larger than those of correct condition in Pe ($F(2,22)=13.172$, $P<0.001$)

and N450 period ($F(2,22)=13.101$, $P<0.001$). Similar results were obtained in the theta band. As to the ITCs in the alpha band, the statistical significance mainly appeared in ERN ($F(2,22)= 12.752$, $P<0.001$) and Pe ($F(2,22)=42.076$, $P<0.001$) time window. Therefore, the ITC differences induced by the prediction deviants are mainly located in the low-frequency band.

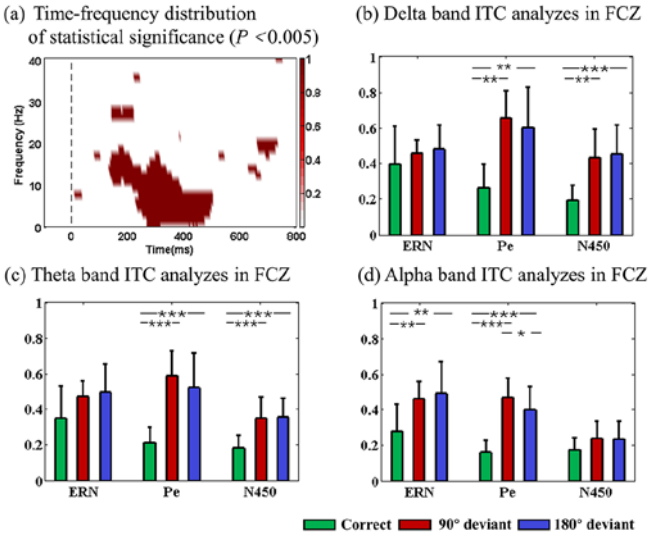

Figure 5. (a) FCZ time-frequency distribution of statistical significance ($P < 0.005$). (b) FCZ ITC analyzes in ERN, Pe, N450 period and 7~13Hz frequency band. (c) PZ time-frequency distribution of statistical significance($P = 0.005$). (d) PZ ITC analyzes in ERN, Pe, N450 period and 7~13Hz frequency band. *presented $0.01<p<0.05$, **presented $0.001<p<0.01$, ***presented $p<0.001$.

C. Classification results

Table 2. the accuracy rate of classifying the three kinds of events in pairs.

Subject	0-180	0-90	90-180
1	90.50%	90.50%	72.00%
2	78.00%	76.50%	65.00%
3	81.50%	78.50%	54.50%
4	92.50%	92.50%	68.00%
5	79.50%	72.50%	68.50%
6	94.50%	83.50%	64.50%
7	83.50%	89.50%	63.50%
8	91.00%	94.50%	60.50%
9	87.50%	92.50%	56.00%
10	95.00%	83.00%	73.00%
11	89.00%	82.50%	67.50%
12	90.50%	87.00%	64.50%
mean	87.75%	85.25%	64.79%

To test the separability of the ErrPs induced by prediction deviants, the DCPM was used for classification. As shown in Table2, the averaged accuracy rate between Correct-90° deviant, Correctness-180° , 90° -180° deviant was 87.75%, 85.25%, 64.79%, respectively, confirming the separability.

Ⅳ Conclusion

This study probed into the EEG signatures induced by prediction deviants with varying degrees. By analyzing the ERP and ITC, we found the signatures of ERN and N450 could be modulated significantly by the degrees of prediction deviants, and such difference mainly resulted from the ITC changes in the low-frequency band (<13Hz). Moreover, by the assistant of the DCPM, the separability of the EEG features induced by varying degree deviants was confirmed. The results can provide new neural evidence for better understanding the ErrP signatures, and contribute to making better use of ErrP for developing BCIs.

References

[1] Lebedev M A, Nicolelis M. Brain-machine interfaces: past, present and future[J]. Trends in Neurosciences, 2006, 29(9): 536-546.

[2] Wolpaw J R, Wolpaw E W. Brain-computer interfaces: principles and practice[M]. OUP: New York, NY, USA, 2012.

[3] Townsend G, Platsko V. Pushing the P300-based brain–computer interface beyond 100 bpm: Extending performance guided constraints into the temporal domain[J]. Journal of neural engineering, 2016, 13(2): 026024.

[4] Chen X, Wang Y, Nakanishi M, et al. High-speed spelling with a noninvasive brain–computer interface[J]. Proceedings of the national academy of sciences, 2015, 112(44): E6058-E6067.

[5] Nakanishi M, Wang Y, Chen X, et al. Enhancing detection of SSVEPs for a high-speed brain speller using task-related component analysis[J]. IEEE Transactions on Biomedical Engineering, 2017, 65(1): 104-112.

[6] Wang K, Wang Z, Guo Y, et al. A brain-computer interface driven by imagining different force loads on a single hand: an online feasibility study[J]. Journal of neuro engineering and rehabilitation, 2017, 14(1): 93.

[7] Kappenman E S, Steven J L. The Oxford handbook of event-related potential[M]. Oxford University Press: New York, NY, USA, 2012; pp. 231–238.

[8] Chavarriaga R, Sobolewski A, Millán J. Errare machinale est: the use of error-related potentials in brain-machine interfaces[J]. Frontiers in Neuroscience, 2014, 8:208.

[9] Zander T O, Krol L R, Birbaumer N P, et al. Neuroadaptive technology enables implicit cursor control based on medial prefrontal cortex activity[J]. Proceedings of the National Academy of Sciences of the United States of America, 2017, 113(52):14898–14903.

[10] Harty S, Murphy P R, Robertson I H, O'Connell R G. Parsing the neural signatures of reduced error detection in older age[J]. Neuroimage, 2017, 161: 43–55.

[11] Rao R P, Ballard D H. Predictive coding in the visual cortex: a functional interpretation of some extra-classical receptive-field effects[J]. Nature Neuroscience, 1999, 2(1):79-87.

[12] De L, Micha H, Peter K. How do expectations shape perception?[J]. Trends in Cognitive Sciences, 2018, 22: 764–779.

[13] Somon B, Campagne A, Delorme A, Berberian B. Human or not human? Performance monitoring ERPs during human agent and machine supervision[J]. NeuroImage, 2019, 186: 266–277.

[14] Cruz A, Pires G, Nunes U J. Double ErrP detection for automatic error correction in an ERP-based BCI speller[J]. IEEE transactions on neural systems and rehabilitation engineering, 2018, 26(1): 26–36.

[15] Krol L R, Haselager P, Zander T O. Cognitive and affective probing: a tutorial and review of active learning for neuroadaptive technology[J]. Journal of neural engineering, 2020, 17(1): 012001.

[16] Wirth C, Dockree P M, Harty S, Lacey E, Arvaneh M. Towards error categorisation in BCI: single-trial EEG classification between different errors[J]. Journal of neural engineering, 2019, 17(1): 016008.

[17] Yousefi R, Rezazadeh Sereshkeh A, Chau T. Development of a robust asynchronous brain-switch using ErrP-based error correction[J]. Journal of neural engineering, 2019, 16(6): 066042.

[18] Xu M, Xiao X, Wang Y, et. al. A brain–computer interface based on miniature-event-related potentials induced by very small lateral visual stimuli. IEEE Trans. Biomed. Eng. 2018, 65: 1166–1175.

[19] Wacongne C, Changeux J P, Dehaene S. A neuronal model of predictive coding accounting for the mismatch negativity[J]. The Journal of neuroscience: the official journal of the Society for Neuroscience, 2012, 32(11): 3665–3678.